Effect of Substitution on the Hole Mobility of Bis(diarylamino)biphenyl Derivatives Doped in Poly(Styrene)

José-Luis Maldonado,[†,§] Maximilienne Bishop,[‡] Canek Fuentes-Hernandez,[†] Pascal Caron,[†] Benoit Domercq,[†] Ya-Dong Zhang,[‡] Stephen Barlow,[‡] S. Thayumanavan,[‡] Massimo Malagoli,[‡] Jean-Luc Brédas,[‡] Seth R. Marder,[†,‡] and Bernard Kippelen*[,†]

Optical Sciences Center, and Department of Chemistry, University of Arizona, Tucson, Arizona 85721

Received August 13, 2002. Revised Manuscript Received December 30, 2002

The effect of substitution on hole mobility in *N*,*N*′-bis(*m*-tolyl)-*N*,*N*′-diphenyl-1,1′-biphenyl-4,4′-diamine (TPD) derivatives doped in polystyrene was studied using the time-of-flight technique. Mobility data were collected as a function of electric field and temperature to yield the energetic and positional disorder parameters defined in the disorder formalism. Substituted derivatives exhibit lower mobilities than regular TPD. This decrease is influenced by the change in dipole moment upon substitution of the molecule. However, the dipolar disorder contribution is found to account only partially for the large differences in mobility.

Introduction

There has been considerable interest in charge-transport phenomena in semiconducting doped polymers in recent years due to their widespread use in xerography,[1,2] electroluminescent devices (OLEDs),[3−5] photovoltaic cells,[6,7] and photorefractive systems.[8] Their range of application is continuously widening. In many applications, these materials are combined with other organic molecules or with metallic electrodes; it is, therefore, important to be able to control the relative frontier orbital energies, that is, the energies of the highest occupied molecular orbital (HOMO) or the lowest unoccupied molecular orbital (LUMO) (which correlate with the ionization potential and the electron affinity, respectively). For hole-transport materials, the energy of the HOMO with respect to the vacuum (which can be estimated from ionization potential data) is the most relevant parameter. Recent advances in methodologies for synthesis of triarylamine compounds have made possible the synthesis of a variety of new substituted molecules.[9−12] Several derivatives of the well-known hole-transport material *N*,*N*′-bis(*m*-tolyl)-*N*,*N*′-diphenyl-1,1′-biphenyl-4,4′-diamine (TPD) (see Figure 1) have been developed.[11−17] Tuning of the ionization potential in TPD-based molecules is usually achieved by substituting the external aryl groups with electron-withdrawing and electron-donating moieties. However, as the ionization potential is altered by substitution, the geometric and electronic properties of the molecule are changed simultaneously, potentially influencing fundamental physical processes such as charge mobility.[18] The effects of tailoring the electronic structure of these molecules on the charge mobility is, therefore, of interest for the development of new organic optoelectronic materials and devices.

For the present work, three derivatives of TPD with various substituents and ionization potentials were synthesized. Alkoxy substituents in the para position of the external aryl groups (compounds **I** and **II** in

* To whom correspondence should be addressed. Tel.: 520-621-4341. Fax: 520-626-4221. E-mail: kippelen@u.arizona.edu.
† Optical Sciences Center, University of Arizona.
‡ Department of Chemistry, University of Arizona.
§ Permanent address: Centro de Investigaciones en Óptica A.P. 1-948, 37000 León, Gto., México. Postdoctoral visit: CONACyT Grant 010144.

(1) Borsenberger, P. M.; Weiss, D. S. *Organic Photoreceptors for Xerography*; Marcel Dekker: New York, 1998.
(2) Pai, D. M.; Springett, B. E. *Rev. Mod. Phys.* **1993**, *65*, 163.
(3) Tang, C. W.; VanSlyke, S. A. *Appl. Phys. Lett.* **1987**, *51*, 913.
(4) Sheats, J. R.; Antoniadis, H.; Hueschen, M.; Leonard, W.; Miller, J.; Moon, R.; Roitman, D.; Stocking, A. *Science* **1996**, *273*, 884.
(5) Friend, R. H.; Gymer, R. W.; Holmes, A. B.; Burroughes, J. H.; Marks, R. N.; Taliani, C.; Bradley, D. D. C.; Dos Santos, D. A.; Bredas, J. L.; Logdlund, M.; Salaneck, W. R. *Nature* **1999**, *397*, 121.
(6) Yu, G.; Gao, J.; Hummelen, J. C.; Wudl, F.; Heeger, A. J. *Science* **1995**, *270*, 1789.
(7) Halls, J. J. M.; Walsh, C. A.; Greeham, N. C.; Marseglia, E. A.; Friend, R. H.; Moratti, S. C.; Holmes, A. B. *Nature* **1995**, *376*, 498.
(8) Kippelen, B.; Marder, S. R.; Hendrickx, E.; Maldonado, J. L.; Guillemet, G.; Volodin, B. L.; Steele, D. D.; Enami, Y.; Sandalphon; Yao, Y. J.; Wang, J. F.; Rockel, H.; Erskine, L.; Peyghambarian, N. *Science* **1998**, *279*, 54.
(9) Wolfe, J. P.; Wagaw, S.; Buchwald, S. L. *J. Am. Chem. Soc.* **1996**, *118*, 7215.
(10) Thayumanavan, S.; Barlow, S.; Marder, S. R. *Chem. Mater.* **1997**, *9*, 3231.
(11) Okumoto, K.; Wayaku, K.; Noda, T.; Kageyama, H.; Shirota, Y. *Synth. Met.* **2000**, *111−112*, 473.
(12) Shirota, Y.; Okumoto, K.; Inada, H. *Synth. Met.* **2000**, *111−112*, 387.
(13) Shi, J.; Tang, C. W. *Appl. Phys. Lett.* **1997**, *70*, 1665.
(14) O'Brien, D. F.; Burrows, P.; Forrest, S. R.; Koene, B. E.; Loy, D.; Thompson, M. E. *Adv. Mater.* **1998**, *10*, 1108.
(15) Koene, B. E.; Loy, E.; Thompson, M. E. *Chem. Mater.* **1998**, *10*, 2235.
(16) Bellmann, E.; Shaheen, S. E.; Thayumanavan, S.; Barlow, S.; Grubbs, R. H.; Marder, S. R.; Kippelen, B.; Peyghambarian, N.*Chem. Mater.* **1998**, *10*, 1668.
(17) Bellmann, E.; Shaheen, S. E.; Grubbs, R. H.; Marder, S. R.; Kippelen, B.; Peyghambarian, N. *Chem. Mater.* **1999**, *11*, 399.
(18) Bender, T. P.; Graham, J. F.; Duff, J. M. *Chem. Mater.* **2001**, *13*, 4105.

10.1021/cm0207907 CCC: $25.00
Published on Web 02/01/2003

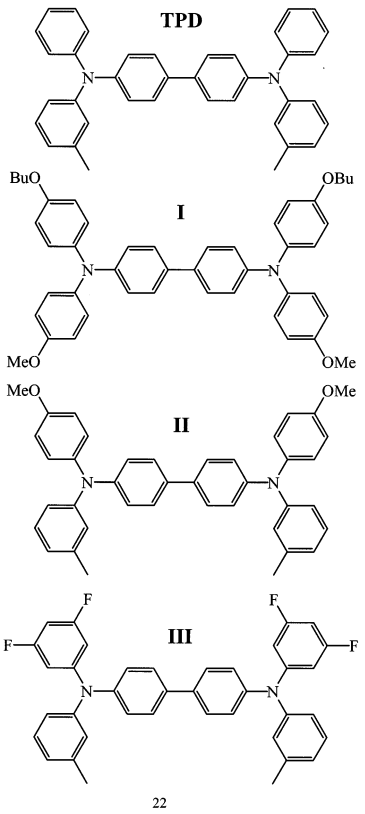

Figure 1. Structures of the substituted bis(diarylamino)-biphenyl derivatives studied in this work.

Figure 1) yield molecules with an ionization potential lower than that of TPD. Fluorine atoms (in the case of compound **III**, Figure 1, in the meta positions) have the opposite effect. Note that **I** and **II** differ by the size and number of their alkoxy substituents.

In our studies, molecules **I**, **II**, **III**, and regular TPD were doped, at the same concentration, into a polystyrene matrix and their hole-transport properties were studied by the time-of-flight technique. This technique allows for the direct measurement of charge-carrier mobilities. Many recent transport studies in doped polymers and molecular glasses have been analyzed using the disorder formalism developed by Bässler, Borsenberger, and co-workers.[19−21] In the disorder formalism, it is assumed that charge transport occurs by hopping through a manifold of localized states with superimposed energetic and positional disorder. The distributions of hopping site energies and distances are Gaussian and characterized by their width σ and Σ, respectively. A key prediction of the model is that mobility decreases when increasing the energetic disorder width σ and that a random distribution of molecules with a permanent dipole moment contributes significantly to this disorder. In an earlier work,[22] we studied theoretically the impact of substitution on the geometry and electronic structure of TPD derivatives and found that substitution can increase the dipole moment of a TPD-based molecule by up to nearly 1 order of magnitude. Here, we investigate, through time-of-flight experiments, the effects of substitution on the mobility and compare the results to those predicted from the dipole moment calculations in the framework of the disorder formalism.

(19) Bässler, H. *Phys. Status Solidi B* **1993**, *175*, 15.
(20) Borsenberger, P. M.; Magin, E. H.; van der Auweraer, M.; de Schryver, F. C. *Phys. Status Solidi A* **1993**, *140*, 9.
(21) Bässler, H. *Mol. Cryst. Liq. Cryst.* **1994**, *252*, 11.
(22) Malagoli, M.; Manoharan, M.; Kippelen, B.; Bredas, J. L *Chem. Phys. Lett.* **2002**, *354*, 283.

Table 1. First Oxidation Potentials and Estimated Values of Ionization Potentials of the Molecules Described in This Study

molecule	oxidation potential[a] (mV)	ionization potential (eV)
TPD	+380	5.5
I	+170	5.3
II	+280	5.4
III	+575	5.7

[a] Halfwave potentials measured versus ferrocenium/ferrocene in tetrahydrofuran (THF).

Experimental Section

Synthesis. TPD was used as supplied by Aldrich. The TPD derivatives **II** and **III** were synthesized as described previously.[10]

Compound I. 4,4′-Dibromobiphenyl (20.0 g, 64 mmol) was added to a solution of $Pd_2(dba)_3$ (0.90 g, 0.98 mmol) and DPPF (0.84 g, 1.52 mmol) in toluene (100 mL) and the mixture was stirred for 10 min under nitrogen. Sodium *tert*-butoxide (13.7 g, 128 mmol) and 4-*n*-butoxyaniline (22.0 g, 133 mmol) were added to the stirred solution and the reaction mixture was heated to 90 °C for 6 h. After the mixture was cooled to room temperature, the crude product (28.4 g) was collected by filtration, washed with methanol and water, and dried under reduced pressure. A portion of the crude 4,4′-bis[(4-*n*-butoxyphenyl)amino]biphenyl (5.0 g) was combined with 4-iodoanisole (5.5 g, 23.8 mmol), copper powder (7.2 g), potassium carbonate (20.0 g), and 18-crown-6 (300 mg) in 1,2-dichlorobenzene (30 mL) and heated to 130 °C for 20 h under nitrogen. Solids were removed by filtration and the solvent was removed under reduced pressure; the product was purified by column chromatography on silica gel using toluene/ethyl acetate (9:1) as eluent to give 6.1 g of the product (8.8 mmol, 78%). ^{1}H NMR (250 MHz, acetone-d_6): δ 7.24 (d, 4H, J = 8.7 Hz), 7.04 (d, 4H, J = 9.0 Hz), 7.03 (d, 4H, J = 9.0 Hz), 6.88 (m due to overlapping peaks, 12H), 3.97 (t, 4H, J = 6.4 Hz), 3.77 (s, 6H), 1.73 (m, 4H), 1.49 (m, 4H), 0.96 (t, 6H, J = 7.3 Hz). ^{1}H NMR (250 MHz, benzene-d_6): δ 7.45 (d, 4H, J = 8.7 Hz), 7.19−7.09 (m due to overlapping peaks, 12H), 6.79 (d, 4H, J = 9.0 Hz), 6.73 (d, 4H, J = 8.9 Hz), 3.61 (t, 4H, J = 6.3 Hz), 3.29 (s, 6H), 1.56 (m, 4H), 1.34 (m, 4H), 0.82 (t, 6H, J = 7.3 Hz). ^{13}C NMR (62.5 MHz, benzene-d_6): δ 156.4, 156.0, 148.1, 141.7, 141.6, 133.9, 127.5, 126.8, 126.7, 122.0, 155.7, 115.1, 67.8, 55.0, 31.7, 19.5, 13.9. FAB HRMS calcd for $C_{46}H_{48}N_2O_4$: 692.3614. Found: 692.3606. Anal. Calcd for $C_{46}H_{48}N_2O_4$: C, 79.74; H, 6.98; N, 4.04. Found: C, 79.84, H, 7.04; N, 4.08.

Cyclic Voltammetry. Cyclic voltammetry was performed on a BAS 100*B* potentiostat equipped with a nonaqueous Ag/AgCl pseudo-reference electrode, a glassy-carbon working electrode, and a platinum auxiliary electrode. Samples were analyzed in 0.2 M tetrabutylammonium hexafluorophosphate tetrahydrofuran solutions using the ferrocenium/ferrocene couple as an internal reference. Table 1 lists the values of the halfwave potential for the molecular oxidation to the monocation, measured by cyclic voltammetry, and the corresponding values of the ionization potential of the different molecules, estimated by considering that the ionization potential of ferrocene relative to vacuum is 5.15 eV. These values of ionization potential are approximate but do provide a simple way to compare the relative HOMO levels of this series of TPD-based derivatives (for an accurate determination in a situation relevant to device operation, photoemission spectroscopy in the solid state should be performed).

Sample Preparation. TPD samples were prepared by dissolving TPD (50 mg) and PS (50 mg) in dichloromethane.

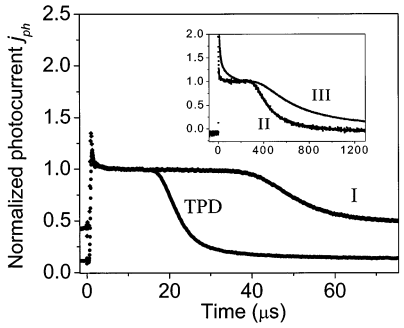

Figure 2. Typical transient photocurrents observed for TPD:PS and **I**:PS composites. Inset: **II**:PS and **III**:PS composites. The applied field was 4×10^5 V/cm and $T = 297$ K. Sample thickness was 10 μm.

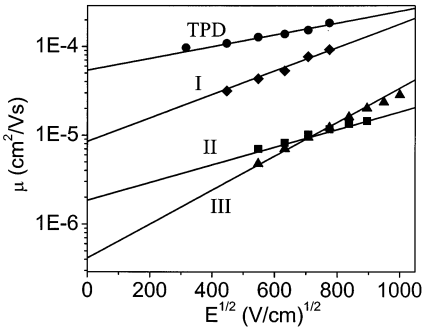

Figure 3. Electric-field dependence of the hole mobility measured in TPD:PS, **I**:PS, **II**:PS, and **III**:PS composites at $T = 297$ K. Symbols represent experimental data and full lines are calculations according to the disorder formalism.

The solution was filtered through a syringe with a 0.2-μm pore size filter. The solvent was evaporated under reduced pressure on a rotary evaporator. The mixture was dried for 24 h in a vacuum oven at 50 °C. Next, the dried material was melted and mixed between two large glass slides to remove trapped air bubbles from the film. This step was repeated several times until the mixture was optically clear and uniform. A small piece of this film was melted between two ITO-coated glass slides at a temperature between 150 and 190 °C. Calibrated glass spacers of 10 μm were used to ensure a uniform sample thickness. Finally, samples were sealed with quick-setting epoxy adhesive. Mixtures with molecules **I** and **II** were prepared analogously but using weighted ratios PS:**I** of 1:1.34 and PS:**II** of 1:1.12 to compensate for the increased molecular weights of the substituted TPDs and yield the same molecular concentration in PS. With molecule **III**, a weighted ratio PS:**III** of 1:1.14 would have provided samples with the same concentration; however, we encountered difficulties in preparing such samples. Molecule **III** yielded polymer composites that exhibited phase separation over time. Hence, we used a weighted ratio PS:**III** of 1:1, which was the highest we could achieve with good reproducibility. This ratio leads to a concentration of hole-transport molecules that is 14% lower compared with that of the other samples.

Time-of-Flight Technique. Hole mobility was measured in air by the conventional time-of-flight method[1,23,24] with the samples mounted inside a temperature-controlled unit. A low-noise high-voltage power supply was used for applying the bias voltage. The photocurrent generated by irradiation with 6-ns pulses from a N_2 laser (337 nm) was amplified using a low-noise preamplifier and monitored with a digital oscilloscope. To keep $RC_p \ll t_t$ (transit time), resistance values were $R = 10^2-10^4\ \Omega$. C_p represents the total capacitance of the electrical circuit. Sample capacitance values were on the order of 10 pF. Neutral density filters were used when necessary to avoid excess charge accumulation in the samples that can create nonuniformity in the electrical field across the sample.

Results and Discussion

Time-of-Flight Results and Analysis. Figure 2 shows typical normalized transient photocurrents (j_{ph}) measured as a function of time (t) at room temperature with an applied field of 4×10^5 V/cm. At most temperatures and applied fields, transient photocurrents were nondispersive and the transit times were determined directly from the linear plot of the transient photocurrent vs time. For dispersive signals, the transit times were determined from the intersection of two straight lines with different slopes at short and long times of the photocurrent transients, in a double logarithmic plot. The hole drift mobility μ was calculated from the transit time t_t according to the equation $\mu = d^2/t_t V$, where d is the sample thickness and V the applied voltage. It was found that the mobility is highest for the regular TPD and decreases when using substituted molecules.

The electric field and temperature dependencies of the measured hole mobilities were analyzed within the framework of the disorder formalism. In this framework, the mobility is given by

$$\mu = \mu_0 \exp\left[-\left(\frac{2\hat{\sigma}}{3}\right)^2\right]\exp[C(\hat{\sigma}^2 - \Sigma^2)E^{1/2}] \qquad (1)$$

where μ_0 is the disorder-free mobility, E is the applied electric field, T is the temperature, C is an empirical constant with a value of 2.9×10^{-4} (cm/V)$^{1/2}$, k_B is the Boltzmann constant, and Σ is the width of the positional disorder distribution. In eq 1, $\hat{\sigma} = \sigma/k_B T$, where σ is the width of the energetical disorder distribution. Hole mobilities were measured in all samples as a function of applied field and temperature to determine the parameters μ_0, σ, Σ, and the value of C for these new molecules doped in PS.

Figure 3 shows the mobilities for all samples measured at room temperature as a function of applied field. The mobility values obtained for samples doped with TPD are consistent with those reported previously in such samples.[1] As shown in Figure 3, in a semilogarithmic representation as a function of the square root of the applied field, the mobility data follow a straight line. This dependence is consistent with the functional dependence of mobility on electric field predicted by the disorder formalism.

To determine the quantities μ_0 and σ, zero-field mobility values are extrapolated from the field-dependent mobility data measured at various temperatures. For each temperature, a plot similar to Figure 3 is generated for each sample and the intercept of the straight line gives the corresponding zero-field mobility. According to eq 1, a semilogarithmic plot of the extrapolated values of the zero-field mobilities $\mu\ (T, E=0)$ as a function of $1/T^2$ yields a straight line with a slope given by $-2\sigma^2/3k_B{}^2$ and an intercept of $\ln(\mu_0)$. These plots are shown in Figure 4 for the four samples investigated in this study. The values of μ_0 and σ determined from the analysis of these plots are summarized in Table 2, along with room-temperature mobilities measured at a field

(23) Spear, W. E. *J. Non-Cryst. Solids* **1969**, *1*, 197.
(24) Melnyk, A. R.; Pai, D. M. In *Physical Methods of Chemistry*, 2nd ed.; Rossiter, B. W., Baetzold, R. C., Eds.; Wiley: New York, 1993; Vol. 8, p 321.

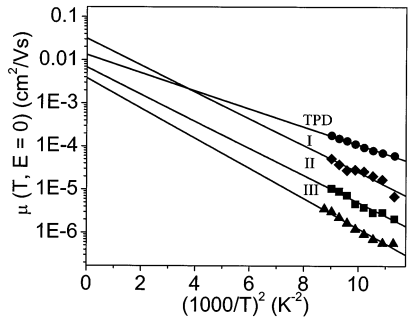

Figure 4. Temperature dependence of the hole mobility for the four composites TPD:PS, **I**:PS, **II**:PS, and **III**:PS extrapolated at zero electric field. Symbols are experimental data and full lines are best fits obtained from linear regressions.

Table 2. Mobility Values and Hole Transport Parameters of the Disorder Formalism Extrapolated from the Analysis of the Field and Temperature Dependence of the Mobility Measured in 10-μm-Thick Samples of PS Doped with Different Molecules

sample composition (weight ratios in parentheses)	μ^a ($cm^2/V\cdot s$)	μ_0 ($cm^2/V\cdot s$)	σ (eV)	C $(cm/V)^{1/2}$	Σ
TPD:PS (1:1)	1.5×10^{-4}	13.12×10^{-3}	0.090	2.67×10^{-4}	2.57
I:PS (1.34:1)	6.3×10^{-5}	31.29×10^{-3}	0.110	5.46×10^{-4}	3.59
II:PS (1.12:1)	8.2×10^{-6}	6.80×10^{-3}	0.110	2.04×10^{-4}	2.69
III:PS (1:1)	6.7×10^{-6}	3.82×10^{-3}	0.116	2.56×10^{-4}	1.83

[a] Measured at $E = 4 \times 10^5$ V/cm and $T = 297$ K.

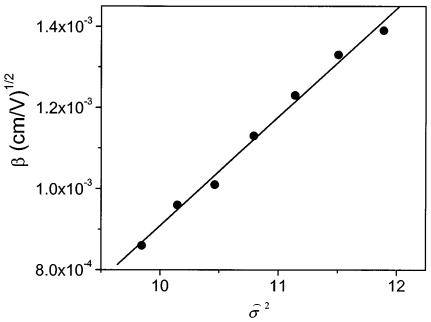

Figure 5. Plot of β vs $\hat{\sigma}^2$ for a composite TPD:PS. Symbols are experimental data and full line is the best fit obtained from a linear regression.

of 4×10^5 V/cm. As expected, substituted TPD molecules lead to larger energetic disorder compared with regular TPD. The energetic disorder is larger for **III**, the fluoro derivative, than for the alkoxy derivatives **I** and **II**.

To obtain the quantities Σ and C, one determines the slopes $\beta = C(\hat{\sigma}^2 - \Sigma^2)$ of the straight lines obtained when plotting the mobility data in a semilogarithmic representation as a function of the square root of the applied field (see Figure 3) at various temperatures. Then, the plot of β vs $\hat{\sigma}^2$ yields a straight line with slope C and intercept $-C\Sigma^2$, from which Σ can be determined. Such a plot for a sample doped with regular TPD is shown in Figure 5. The best fit yields in this case $C = 2.67 \times 10^{-4}$ $(cm/V)^{1/2}$, a value that is close to the empirical value of 2.9×10^{-4} $(cm/V)^{1/2}$ given by the disorder formalism. As predicted by eq 1, values of β decrease with increasing temperature as the effect of trapping due to the energetic disorder decreases; that is, it becomes easier for hopping to occur between molecules with slightly different energies. The random orientation of asymmetric molecules and variations in the intermolecular distances are parametrized as the positional disorder, Σ. The values of C and Σ determined for the four samples are summarized in Table 2. Σ is lowest for polymers doped with compound **III** and is greatest for samples doped with **I**. This large value can be attributed to the length of the flexible substituents, in particular, the butoxy chains. Note that except for the **I**:PS composite all the values derived for C are close to the empirical value of 2.9×10^{-4} $(cm/V)^{1/2}$. To check the consistency of the disorder parameters derived from our analysis for the four composites, we have calculated the field dependence of the mobility according to eq 1 with the parameters listed in Table 2 for each sample. The result of these calculations are shown as full lines in Figure 3 and are in good agreement with the experimental mobility data.

Dipolar Contribution to the Energetic Disorder. It is well-established that the width of the energy distribution of the hopping sites σ is strongly dependent on the dipole moment of the dopant molecule as well as the polymer repeat unit. The argument is that a random distribution of dipoles generates fluctuations in electrostatic potential that add to the effects resulting from van der Waals interactions. The total width can be expressed as a sum of independent contributions,[25−28]

$$\sigma^2 = \sigma_d^2 + \sigma_{vdW}^2 + \sigma_D^2 \qquad (2)$$

where σ_d is the contribution due to dipolar properties of the dopant molecule, σ_{vdW} is the van der Waals contribution, and σ_D is the dipolar contribution due to dipolar effects introduced by the polymer matrix. Since the dipole moment of PS is near-zero, the polymer dipolar component, σ_D, can be neglected here. The dipolar component σ_d can be estimated by expressions derived by Dieckmann and co-workers[29] and Young,[30]

$$\sigma_d = \frac{k_0 c^n p}{a^2 \epsilon} \qquad (3)$$

where c is the fraction of lattice sites occupied by dipoles[26] (around 0.5 in our case), p is the dipole moment (in Debye), α is the distance between two transport molecules (in Å), ϵ is the relative dielectric constant, and $k_0 = 3.06$ and $n = {}^2/_3$ in Dieckmann's expression and $k_0 = 7.05$ and $n = {}^1/_2$ in Young's expression. The numerical predictions from eq 3 due to Young are generally twice those obtained from Dieckmann's expression. From the lattice gas model, $\alpha = (M_w/N_A c\rho)^{1/3}$, where M_w is the molecular weight of the TPD-based dopant molecule, N_A is the Avogadro number, and ρ is the sample mass density. All these quantities for samples doped with either TPD, molecule **II**, or molecule **III** are summarized in Table 3. The dielectric constants were determined by measuring the sample capacitance. For the mass density, we used a value of $\rho = 1.16$ g/cm^3 that was previously reported for TPD.[26,31]

(25) Heun, S.; Borsenberger, P. M. *Chem. Phys.* **1995**, *200*, 245.
(26) Heun, S.; Borsenberger, P. M. *Physica B* **1995**, *216*, 43.
(27) Borsenberger, P. M.; O'Regan, M. B. *Chem. Phys.* **1995**, *200*, 257.
(28) Borsenberger, P. M.; Gruenbaum, W. T.; Magin, E. H.; Sorriero, L. J. *Chem. Phys.* **1995**, *195*, 435.
(29) Dieckmann, A.; Bässler H.; Borsenberger, P. M. *J. Chem. Phys.* **1993**, *99*, 8136.
(30) Young, R. H. *Philos. Mag. B* **1995**, *72*, 435.

Table 3. Sample Composition, Molecular Weight of Dopant Molecule (M_w), Lattice Constant *a*, Dielectric Constant ϵ, Total Width σ of Energetical Disorder, Average Value of Dipole Moment Calculated for Various Conformers in Ref 22, Calculated Dipolar Contribution σ_d to the Energetical Disorder, and Calculated van der Waals Contributions σ_{vdW}

sample composition (weight ratios in parentheses)	M_w (dopant) (g/mol)	a (Å)	ϵ	σ (eV)	$\bar{p}$ (D)	σ_d (eV)	σ_{vdW} (eV)
TPD:PS (1:1)	516	11.4	4.9	0.090	0.46	0.003	0.090
II:PS (1.12:1)	576	11.8	2.5	0.110	1.49	0.021	0.108
III:PS (1:1)	588	11.9	3.6	0.116	2.95	0.029	0.112

In an earlier study,[22] we described theoretically the impact of substitution and molecular conformation on the electronic properties of bis(diarylamino)biphenyl molecules. We pointed out that TPD molecules could adopt six different conformations with very similar total energies and, consequently, that a mixture of these conformers has to be expected in the amorphous solid state. The major difference between conformers was found to be in their dipole moments; their ionization potentials were calculated to be very similar. Similar studies were performed on various substituted TPD derivatives and showed that substitution has an important impact on the dipole moments of the different molecules. The dipole moments of TPD and of molecules **II** and **III** were calculated[22] using quantum mechanical calculations performed at the Hartree−Fock semiempirical and density functional theory (DFT) levels. In the case of TPD, calculations were performed on all six different conformers and yielded DFT values of the dipole moment ranging between 0.147 and 0.719 D, depending on the conformer. For the substituted molecules, the dipole moment values were calculated only for two of the three possible cis or trans conformers. For the four conformers of molecule **II**, the DFT dipole moments were in the range 0.762−2.338 D and for molecule **III** in the range 1.813−4.448 D. To calculate the dipolar contributions to the energetical disorder using eq 3, we took the average of the dipole moment values obtained from the DFT calculations for all conformers.[22] The corresponding values for molecules **II** and **III** and for TPD are summarized in Table 3 (note that calculated values of dipole moment for molecule **I** were not available). Clearly, the dipole moment grows significantly with substitution in **II** and **III**, up to a 7-fold increase in the case of molecule **III** with respect to that of regular TPD. The calculated values of σ_d using Young's formula (eq 3 with $k_0 = 7.05$ and $n = {}^1/_2$) are also shown in Table 3.

From the calculated values of σ_d, we can extrapolate the van der Waals contribution. In the case of TPD, the width of the energetical disorder distribution is largely dominated by the van der Waals contribution, as was previously reported in other studies.[26] The relative contribution of the dipolar disorder to the total width $(\sigma_d/\sigma)^2$ is only 0.1%. Note that the same argument holds for TPD when the dipolar contribution is calculated with the reported experimental value of its dipole moment of 1.52 D.[26] In this case, the contribution is 2%. For polymers doped with substituted molecules **II** and **III** that have higher dipole moments, the dipolar contribution reaches 4% and 6%, respectively. Even in this case, the total width of the density of states is mainly dominated by the van der Waals contribution. The nearly constant value of $\sigma_{vdW} \approx 0.11$ eV measured for polymers doped with molecules **II** and **III** is in good agreement with those reported for a wide range of triarylamine molecules.[26] Our results further support the argument that the van der Waals contribution is independent of the dipole moment for substituted molecules with large dipole moments in the range examined here. However, an important difference is observed between regular TPD and its derivatives.

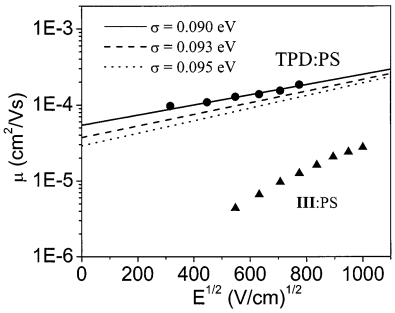

Figure 6. Experimental mobility values measured for composites of TPD:PS (circles) and **III**:PS (triangles). Straight lines are calculated values of the mobility using eq 1 with the parameters $\mu_0 = 13.16$ cm^2/Vs, $C = 2.67 \times 10^{-4}$ (cm/V)$^{1/2}$, and $\Sigma = 2.57$. For each calculated curve the parameter σ was varied from $\sigma = 0.090$ eV (full line), to $\sigma = 0.093$ eV (dashed line), and to $\sigma = 0.095$ eV (dotted line).

On the basis of these results, one might ask if the significant differences observed in the mobility values for materials doped with various substituents can be accounted for solely by the change in dipole moment caused by substitution. In Figure 6, we have plotted the calculated mobility for TPD-doped samples using the parameters reported in Table 2 together with hypothetical mobility values obtained by increasing the width of the energetical disorder σ. For the hypothetical mobility calculations, the parameters μ_0, C, and Σ derived for TPD were kept constant and the width of the energetical disorder σ was increased to 0.093 and 0.095 eV. These values were calculated according to eq 2 using the van der Waals contribution σ_{vdW} of regular TPD ($\sigma_{vdW} = 0.090$ eV) and the calculated values of the dipolar contribution $\sigma_d = 0.021$ and 0.029 eV for molecules **II** and **III**, respectively. Figure 6 clearly shows that the increase in dipole moment alone does not account for the decrease in mobility measured experimentally. This indicates that other effects caused by substitution have to be considered, such as an increase of the van der Waals contribution and changes in pre-exponential mobility factors and in the positional disorder.

In a recent study,[18] it was suggested that the xerographic properties of triarylamines such as hole mobility correlated with the Hammett parameter of the substituent used to quantify the HOMO energy level and the oxidation potential. Substituents have a positive Hammett parameter if they have electron-widthdrawing properties, leading to an increase of the oxidation potential; electron-donating substituents which lower the oxidation potential have negative Hammett parameters. Time-of-flight measurements[18] on substituted triarylamines in a polycarbonate matrix suggested that

(31) Schreiber, A.; Zilker, S. J.; Haarer, D. *J. Chem Phys.* **2000**, *112*, 7190.

the mobility was lower in materials with increasing Hammett parameter and that materials with negative Hammet parameters possessed favorable transport properties. The results of our study point to the conclusion that the best mobility values are obtained in the parent compound with Hammett parameter close to zero and that substitution in all cases reduces the hole mobility. At low fields, the lowest mobilities are observed in the material substituted with electron-withdrawing groups. However, in the high-field region this trend is reversed due to a lower positional disorder in compound **III** compared with **II**.

Conclusions

The hole mobilities of three derivatives of TPD-doped polystyrene with various oxidation potentials doped in PS have been studied by the time-of-flight technique. The hole mobility was the highest in regular TPD and was found to decrease when going from compound **I** to compound **II** and was the lowest at low fields in compound **III**. For all these compounds, the disorder parameters were obtained from the analysis of the field and temperature dependence of the mobility. The observed decrease in mobility with substitution did correlate with an increase of the width of the energetical disorder σ. However, changes in the values of the pre-exponential mobility factor μ_0 and in the width of the positional disorder Σ were also observed. The presence of larger energetic disorder and relatively lower positional disorder for **III** yields a stronger temperature dependence than in the other compounds. The molecular dipole moments of the derivatives increase their energetic disorder, which contributes to their lower mobilities relative to underivatized TPD. However, the key observation of this study is that the increase in the dipolar contribution to the total width of the energetical disorder does not account solely for the significant differences in mobility values observed in substituted TPD molecules.

Acknowledgment. This work was partly funded by NSF through a CAREER grant (B.K.), Grant ECS-0108696 (B.K), and Grant CHE-0078819 (J.L.B.), ONR, AFOSR, NASA, through the University of Alabama at Huntsville, Durel Corp., the State of Arizona through Proposition 301 Initiative, and the IBM Shared University Research program.

CM0207907